



# Gamma-ray emission from isolated and transitional pulsars

Diego F. Torres

Institute of Space Sciences (ICREA & IEEC-CSIC)

*Based on recent research done in collaboration with A. Papitto, D. Viganò, and D. De Martino, K. Hirotani, J. Li, J. Martín, M. Pessah, N. Rea et al.*

*Research done with the support of*





## Outline of the talk

### 1. Considerations for the origin of the gamma-ray emission in transitional pulsars: a propeller model

- Defining the states
- Observational constraints
- Model
- Conclusions

### 2. A synchro-curvature perspective on the generation of the gamma-ray spectra from isolated pulsars

- Synchro-curvature power and the spectra of Fermi-LAT pulsars
- A 1D model to fit spectra
- Correlations
- Conclusions

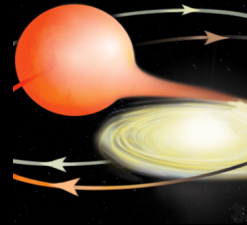
*What relatively simple models can tell about the gamma-ray emission spectra of pulsars in different states?*



## The three stages of transitional pulsars

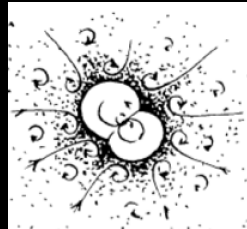
### Accretion powered state

Bright X-ray outburst ( $\sim 10^{36}$  erg/s)  
X-ray pulsations



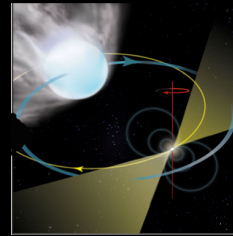
### An intermediate (propeller?) state

Sub-luminous accretion ( $\sim 10^{34}$  erg/s)  
Brighter gamma-ray emission  
X-ray pulsations (10% level)



### Rotation powered state

Faint in X-rays ( $\sim 10^{32}$  erg/s)  
Radio/gamma-ray pulsations





## Limits to accreted matter flow from the detection of pulses

Assuming that the coherent X-ray pulsations observed from PSR J1023+0038 in the disk state were due to accretion of matter onto the NS surface

We can compute a lower (upper) limit to the mass accretion rate onto the NS:  $\dot{M}_{NS}$

- Lower limit: only pulsed luminosity ( $\sim 6\%$  of  $L_x$ ) represents the NS accretion rate
- Upper limit: the total X-ray luminosity  $L_x$  represents the NS accretion rate

$$L_X(0.3 - 79 \text{ keV}) = 7.3 \times 10^{33} \text{ erg s}^{-1}$$

$$5 \times 10^{-14} \text{ M}_{\odot} \text{ yr}^{-1} \simeq (\sqrt{2} A_{rms}) \frac{L_X R_{NS}}{GM_{NS}} < \dot{M}_{NS} < \frac{L_X R_{NS}}{GM_{NS}} \simeq 6 \times 10^{-13} \text{ M}_{\odot} \text{ yr}^{-1}$$

So that  $R_{in}$  is within a factor of a few equal to co-rotation radius, the disk mass accretion should

$$R_{in} = k_m R_A = k_m \left[ \frac{\mu^4}{2GM_* \dot{M}_d^2} \right]^{1/7} < R_c = (GMP^2 / 4\pi^2)^{1/3}$$

$$\dot{M}_d \simeq 7 \times 10^{-11} \text{ M}_{\odot} \text{ yr}^{-1} > 100 \times \dot{M}_{NS}$$

$\gtrsim 99\%$  of the matter in-flowing in the disk must be ejected



## Main ideas for a feasible scenario leading to gamma-emission

- accretion onto the NS surface is inhibited by the propeller effect (i.e.  $R_{lc} > R_{in} > R_c$ );
- electrons are accelerated to relativistic energies at the turbulent boundary between the disk and the propelling magnetosphere;
- relativistic electrons interact with the NS magnetic field lines producing synchrotron emission that explains (at least part of) the X-ray emission;
- synchrotron photons are up-scattered by relativistic electrons, to explain the emission observed in the gamma-ray band.

Natural interpretation of observations

Possible (reconnection, Fermi acc.)

Inevitably, if the former happens

Possible, depending on volume.



# Model build up: energy and mass conservation

$$1 \quad L_{prop} + L_d + \dot{E}_{adv} + L_{NS} + \frac{1}{2} \dot{M}_{ej} v_{out}^2 = \dot{E}_g + N\Omega_*$$

Energy conservation

The energy to power the radiative emission from the disk ( $L_d$ ), the inner disk boundary ( $L_{prop}$ ), the NS surface ( $L_{NS}$ ), the kinetic energy of the outflow ( $\dot{M}_{ej} v^2 / 2$ ), and that converted into internal energy of the flow and advected ( $\dot{E}_{adv}$ )

=

Gravitational energy liberated by in-fall of matter, plus the energy release by the magnetosphere through the torque  $N$

$$\dot{M}_d = \dot{M}_{NS} + \dot{M}_{ej}$$

Mass conservation

the fraction of mass ejected as

$$k_{ej} = \frac{\dot{M}_{ej}}{\dot{M}_d} = 1 - \frac{\dot{M}_{NS}}{\dot{M}_d}$$

$k_{ej} > 0.95$  for PSR J1023+0038

the gravitational energy liberated by the mass in-fall

$$\dot{E}_g = \frac{GM\dot{M}_d}{R_{in}} + GM\dot{M}_{NS} \left( \frac{1}{R_{NS}} - \frac{1}{R_{in}} \right)$$

the NS luminosity is given by efficient conversion of the in-falling grav. energy

$$L_{NS} = GM\dot{M}_{NS} \left( \frac{1}{R_{NS}} - \frac{1}{R_{in}} \right)$$



## Model build up: disk & propeller luminosities

express the disk lum. as a fraction  $\eta$  of the energy radiated by an optically thick, geometrically thin disk

$$L_d = \eta \frac{GM\dot{M}_d}{2R_{in}}$$

The case of a radiatively efficient disk is realized for  $\eta = 1$ .

For values of  $\eta$  lower than unity, the energy that is not radiated by the disk is partly advected, and partly made available to power the propeller emission.

$$\dot{E}_{adv} = (1 - \eta - \xi) \frac{GM\dot{M}_d}{2R_{in}}$$

1

$$L_{prop} + L_d + \dot{E}_{adv} + L_{NS} + \frac{1}{2}\dot{M}_{ej}v_{out}^2 = \dot{E}_g + N\Omega_*$$
$$L_{prop} = \left(\frac{1 + \xi}{2}\right) \frac{GM\dot{M}_d}{R_{in}} + N\Omega_* - \frac{1}{2}k_{ej}\dot{M}_d v_{out}^2$$

Energy conservation



## Model build up: momentum conservation

2

$$\dot{M}_{ej} R_{in} v_{out} = N + \dot{M}_d \Omega_K R_{in}^2$$

Angular momentum conservation at the inner disk boundary

$$\Omega_K = \sqrt{GM/R_{in}^3}$$

Rate of angular momentum in the outflow

=

Torque applied by the magnetic field plus angular momentum carried by disk matter

- Eksi et al. (2005) treated the interaction at the inner disk boundary as a collision of particles, and expressed the outflow velocity as:

$$v_{out} = \Omega_K(R_{in}) R_{in} [1 + (1 + \beta)(\omega_* - 1)]$$

$$\omega_* = \frac{\Omega_*}{\Omega_K(R_{in})} = \left(\frac{R_{in}}{R_{co}}\right)^{3/2}$$

Fastness

$$R_c = (GM_*/\Omega_*^2)^{1/3}$$

- $\beta$  is the elasticity parameter. Anelastic collision is given by  $\beta = 0$ . Elastic case is described by  $\beta = 1$ .



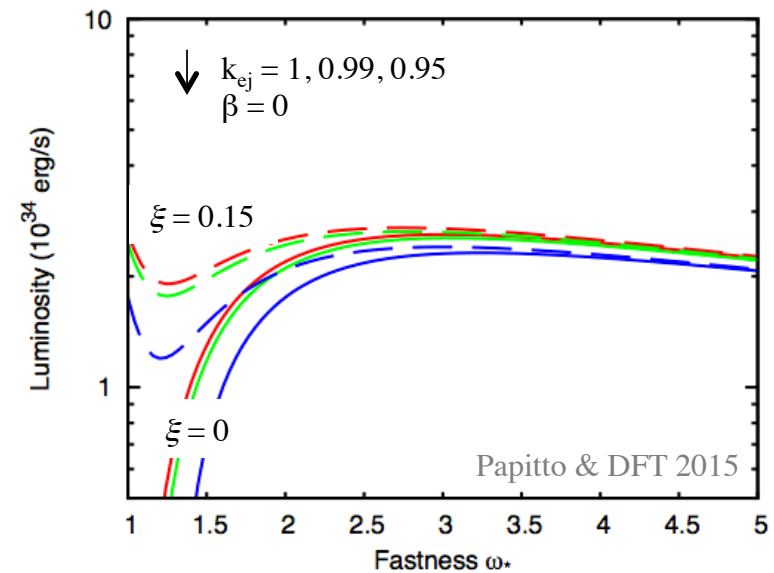
## Luminosity in the needed range

Using the former expressions into the conservation relations

1 2 → Using  $k_{ej} \rightarrow 1$

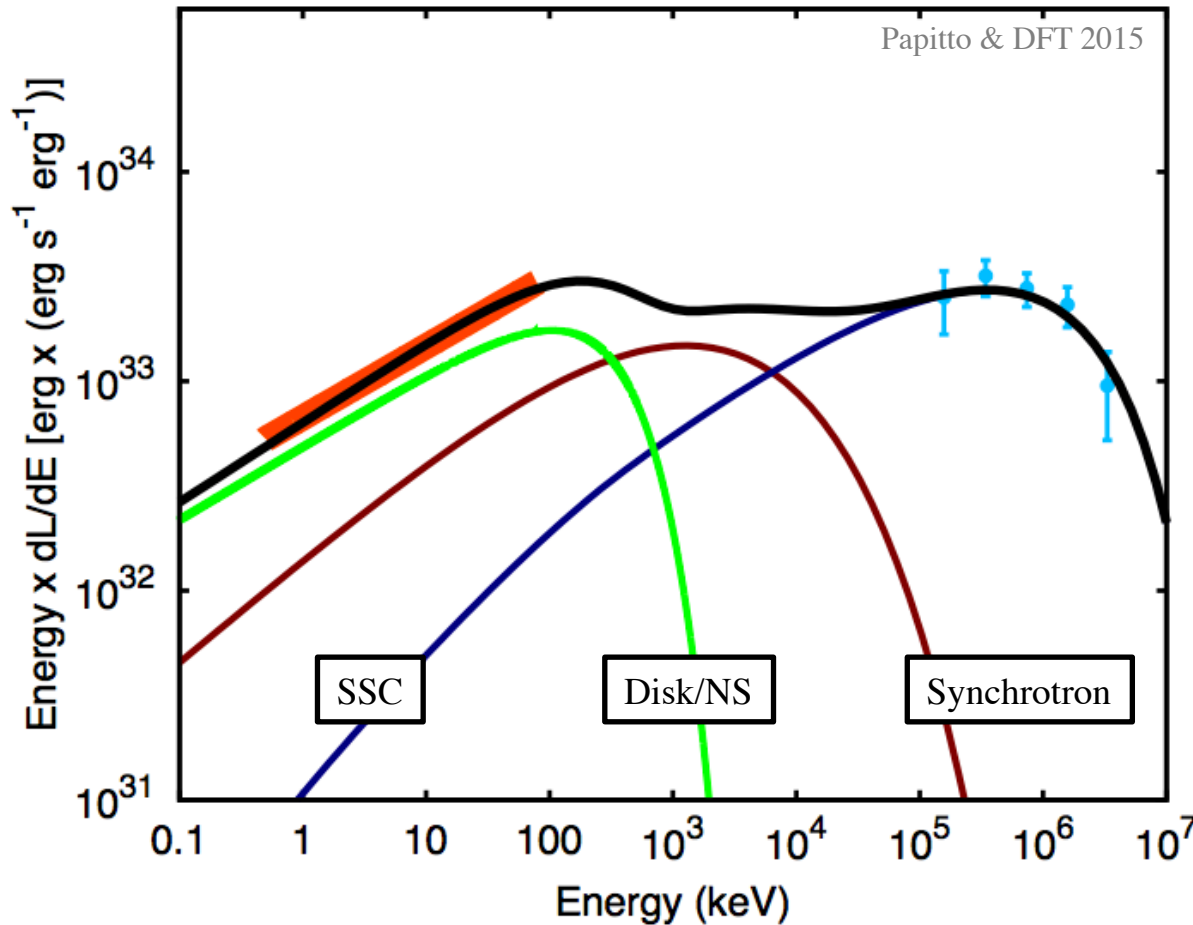
$$L_{prop} = \frac{GM\dot{M}_d}{2R_{in}} [\xi + (\omega_* - 1)^2(1 - \beta^2)]$$
$$= 1.75 \times 10^{35} \omega_*^{-2/3} [\xi + (\omega_* - 1)^2(1 - \beta^2)] \text{ erg s}^{-1}$$

$$N = \dot{M}_d \sqrt{GM R_{in}} \{k_{ej} [\omega_* (1 + \beta) - \beta] - 1\}$$





## Spectral model for PSR J1023-0038



$$\frac{dN_e}{d\gamma} \propto \gamma^{-\alpha} \exp\left(-\frac{\gamma}{\gamma_{max}}\right)$$

$$\bar{B} = \frac{\mu}{R_{in}^3} = \frac{\mu}{R_c^3 \omega_*^2}$$

Gamma-ray emission dominated by self-synchrotron Compton.

Other contributions to IC, e.g., from disk; or brems., are subdominant.

- The parameters of the electron distribution ( $\alpha$ ,  $\gamma_{max}$ ,  $n_e$ ) and the volume  $V$  of the region of acceleration are adjusted to model the gamma-ray emission, for a fixed  $\omega_*$ .
- The contribution of the disk/NS emission in the X-ray band is modelled as a power-law cut at an energy of a few 100 keV, outside the energy band (we chose 300 keV).



## Is a rotation-powered pulsar active... ?

...even in the presence of an accretion disk, with the radio coherent pulsation being washed out by the enshrouding of the system by intra-binary material?

- Particle acceleration could happen in the shock between the pulsar wind of particles and the mass in-flow (Stappers et al. 2014, Coti-Zelati et al. 2014)
- Or from interactions of relativistic electrons in the pulsar wind disk photons, with gamma-emission being inverse Compton produced (Takata et al. 2014, Li et al. 2014)



**Coherent X-ray pulsation:** if not from accretion, the rotationally produced pulsation should be x10 more luminous when the disc is present (extreme mode switching?)



### **spin-down power efficiency**

- X-rays and gamma-rays requires an efficiency of  $\sim 40\%$ ,
- larger than the values typically observed from rotation-powered pulsars,  $0.1\%$  (X-rays, Vink et al. 2011) and  $10\%$  (gamma-rays, Abdo et al. 2013).
- The SED most likely peaks at 1-10 MeV, i.e. if joined by smooth components, a total luminosity equal to  $\sim 1.4 L_{sd}$  is required.
- Flickering in X-rays at hundred-s timescales happens already at  $40\%$  spin-down. Unless fully anti-correlated with gamma-rays, flaring happens beyond this limit.



### **Variability in X-rays?**



## Propeller model conclusions

- Provides a spectrum in agreement with the overall MW scenario
- It also works for XSS J12270 (with similar parameters)
- Impossibility of observationally separating contributions just at the X-ray domain, partially limiting model predictability/testing.
- This gives a large phase space of plausible parameters for the disk component, which can accommodate several different elasticities, radiative efficiencies, etc
- Testable model predictions also happen in a range of energies (few MeV) with currently no sensitive coverage, or at timescales ( $<100$  s) for which Fermi-LAT is not enough sensitive to track them
- This model predicts no detectable TeV counterparts

Model details in  
Papitto & DFT, 2015 ApJ (arXiv 1504.05029)



## Outline of the talk

### 1. A propeller model and considerations for the origin of the gamma-ray emission in transitional pulsars

- Defining the states
- Observational constraints
- Model and caveats
- Conclusions

### 2. A synchro-curvature perspective on the generation of the gamma-ray spectra from isolated pulsars

- Synchro-curvature power and the spectra of Fermi-LAT pulsars
- A 1D model to fit spectra
- Correlations
- Conclusions

*What relatively simple models can tell about the gamma-ray emission spectra of pulsars in different states?*



# Synchro-curvature radiation formulae

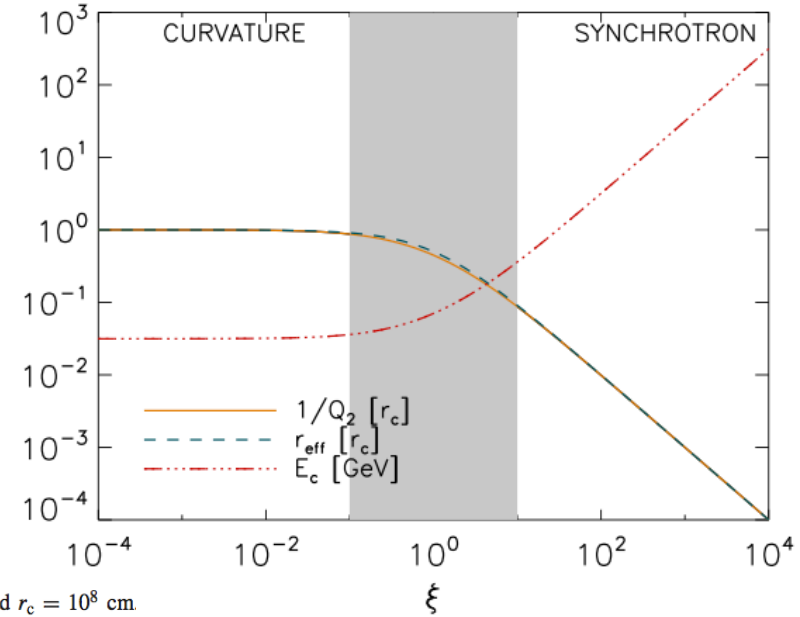
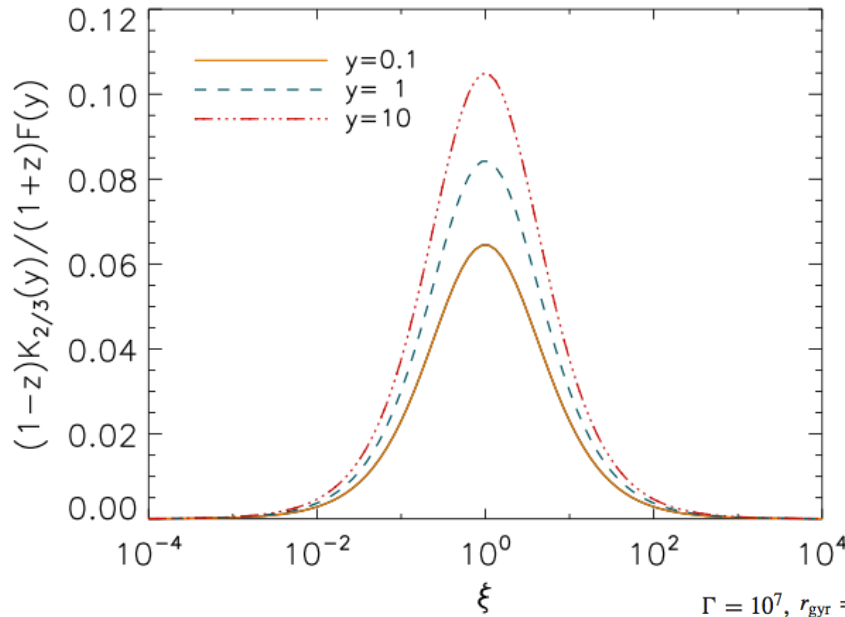
$$\xi = \frac{r_c}{r_{\text{gyr}}} \frac{\sin^2 \alpha}{\cos^2 \alpha} \simeq 5.9 \times 10^3 \frac{r_{c,8} B_6 \sin \alpha}{\Gamma_7 \cos^2 \alpha}$$

The power radiated by one particle per unit energy is

$$\frac{dP_{\text{sc}}}{dE} = \frac{\sqrt{3}(Ze)^2 \Gamma y}{4\pi \hbar r_{\text{eff}}} [(1+z)F(y) - (1-z)K_{2/3}(y)]$$

Where  $K_n$  are the modified Bessel functions of the second kind of index  $n$ , and

$$y(E, \Gamma, r_c, r_{\text{gyr}}, \alpha) \equiv \frac{E}{E_c}, \quad z = (Q_2 r_{\text{eff}})^{-2}, \quad F(y) = \int_y^\infty K_{5/3}(y') dy', \quad r_{\text{eff}} = \frac{r_c}{\cos^2 \alpha} \left(1 + \xi + \frac{r_{\text{gyr}}}{r_c}\right)^{-1}$$





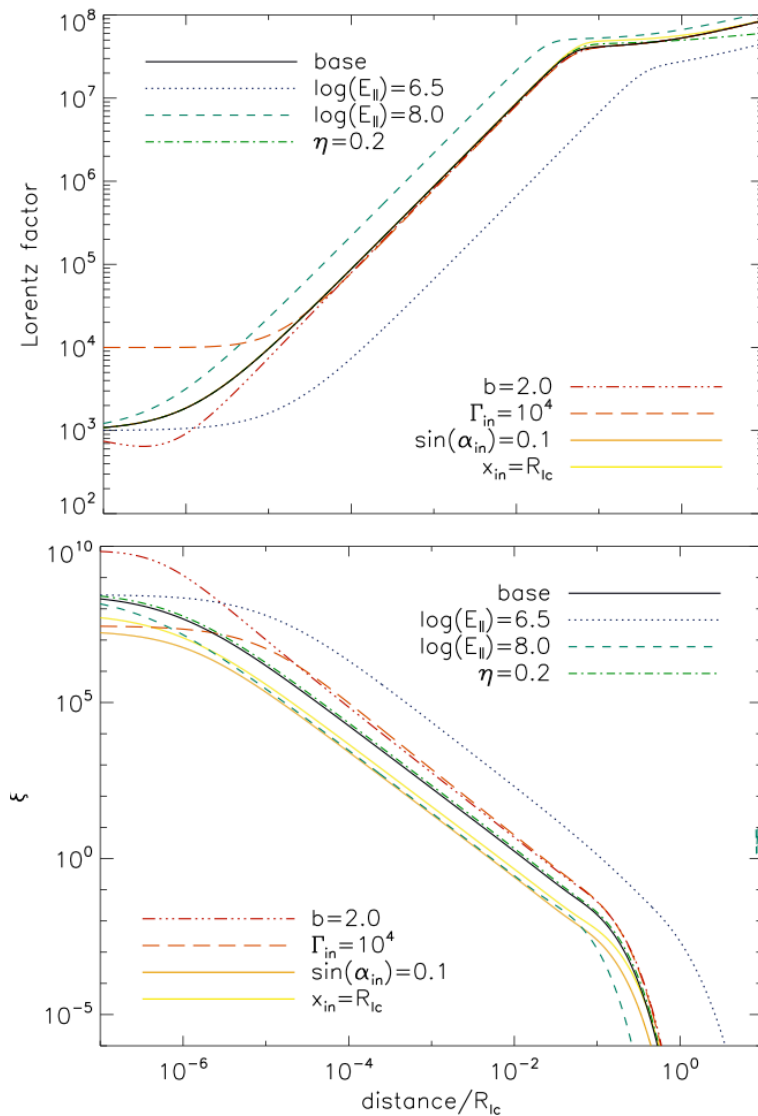
## Particle motion under SC losses balancing with an accelerating $E_{\parallel}$

$$\frac{d\mathbf{p}}{dt} = ZeE_{\parallel}\hat{\mathbf{b}} - \frac{P_{sc}}{v}\hat{\mathbf{p}} \quad \left. \vphantom{\frac{d\mathbf{p}}{dt}} \right\} \begin{aligned} \frac{d(p \sin \alpha)}{dt} &= -\frac{P_{sc} \sin \alpha}{v}, \\ \frac{d(p \cos \alpha)}{dt} &= ZeE_{\parallel} - \frac{P_{sc} \cos \alpha}{v} \end{aligned}$$

- electrons and positrons created by, e.g., pair production  $\Gamma_{in} \sim \frac{E_{\gamma}}{2m_e c^2} \simeq 10^3 E_{\gamma} [\text{GeV}]$
- The pitch angle at birth,  $\alpha_{in}$ , is random  $\alpha_{in} \sim O(1)$  which inevitably implies  $\xi_{in} \gg 1$ .



## Particle trajectories in ‘pulsar gap’, with varying $B, r_c$



- Soon after pair creation,  $\xi \gg 1$ , i.e. losses are dominated by synchrotron
- Then, in a length-scale  $x \ll R_{1c}$ , the electrical acceleration makes  $\Gamma$  increase and  $\sin \alpha$  decrease, until losses are dominated by curvature,  $\xi \ll 1$ .
- $\Gamma_{in}$  and  $\sin \alpha_{in}$  have visible effects in  $\Gamma$  only in the very early part of the trajectories.
- Similarly, the magnetic field dependence only affects the initial part of the evolution. The parameters  $x_{in}$  and  $\eta$  have a negligible influence as well.
- The most relevant parameter is  $E_{\parallel}$ : the larger it is, the larger is  $\Gamma$  and the smaller is  $\xi$ .
- For  $x < 0.1R_{1c}$  the deviations from a purely curvature radiation ( $\xi \ll 1$ ) are important.

The base model (black) has:  $E_{\parallel} = 10^{7.6}$  V/m,  $\eta = 0.5$ ,  $b = 2.5$ ,  $x_{in} = 0.5R_{1c}$ , and the kinetic parameters  $\Gamma_{in} = 10^3$ ,  $\alpha_{in} = \pi/4$ .



## SC power of a particle distribution

The observed spectrum from a ‘pulsar’ is given by the integration *over the population of particles directed to the observer*, along a given accelerating region (the gap):

$$\begin{aligned}\frac{dP_{\text{gap}}}{dE_{\gamma}} &= \int_{x_{\text{in}}}^{x_{\text{out}}} \frac{dP_{\text{sc}}}{dE_{\gamma}} \frac{dN}{dx} dx \\ &= \frac{\sqrt{3}e^2}{2h} y \int_{x_{\text{in}}}^{x_{\text{out}}} \frac{dN}{dx} \frac{\Gamma}{r_{\text{eff}}} \times \\ &\quad [(1+z)F(y) - (1-z)K_{2/3}(y)] dx\end{aligned}$$



## An effective approach for the particle distribution

$$\frac{dP_{\text{gap}}}{dE_{\gamma}} = \int_{x_{\text{in}}}^{x_{\text{out}}} \frac{dP_{\text{sc}}}{dE_{\gamma}} \boxed{\frac{dN}{dx}} dx$$

- e.g., do we see more particles directed towards the observer in the initial or final part of their gap trajectories?
- a number of effects that could justify different weights
  - **geometry**
  - **beaming** is larger at smaller  $\Gamma$ , so that it is easier to detect radiation for less energetic particles.
  - **cascading** is especially produced in the inner gap, where the interactions with X-ray photons are more likely,
- The functional form to represent the distribution is chosen by simplicity, depending on two parameters that are left free: length-scale and normalization

$$\boxed{\frac{dN}{dx}} = N_0 \frac{e^{-(x-x_{\text{in}})/x_0}}{x_0(1 - e^{-x_{\text{out}}/x_0})}$$



## Parameter exploration: reduced to 3 variables

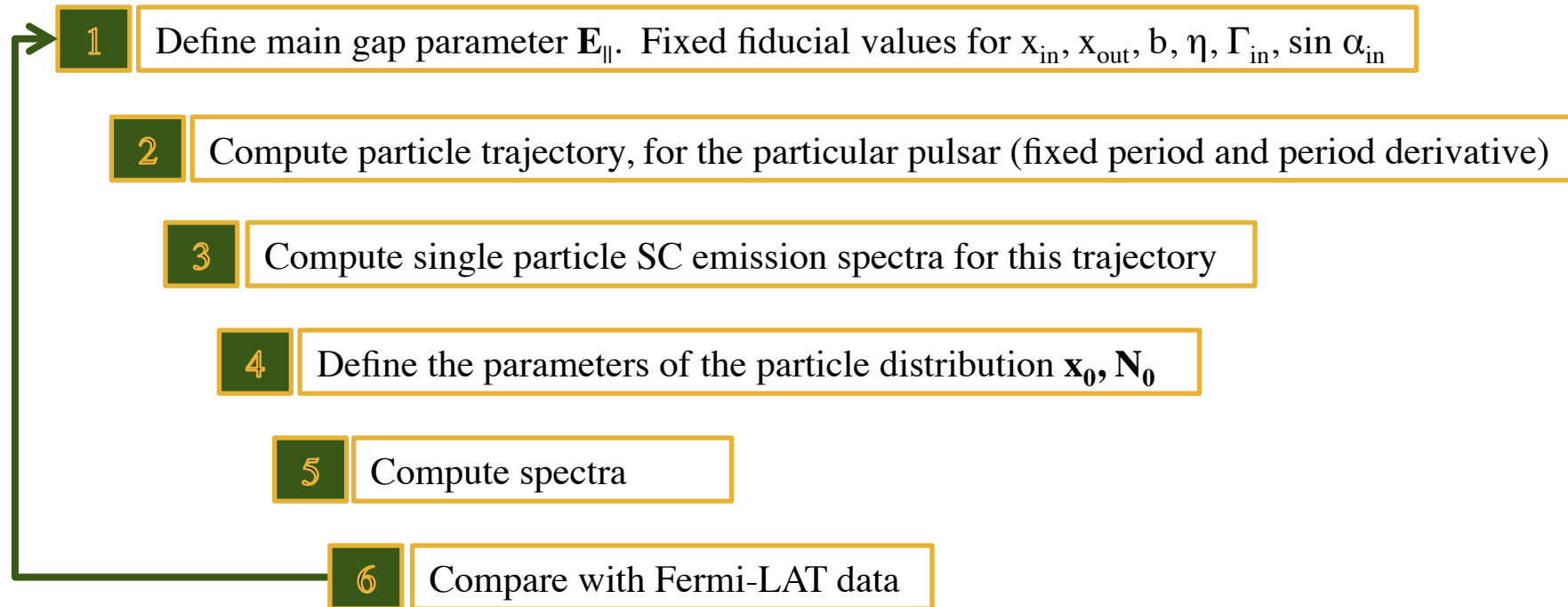
<i>Parameter</i>	<i>Definition</i>	<i>Range</i>	<i>Treatment</i>
$P$	Spin period	1–500 ms	measured
$\dot{P}$	Spin period derivative	$10^{-21}$ – $10^{-12}$	measured
$E_{\parallel}$	Parallel electric field	$10^6$ – $10^{11}$ V/m	fit
$x_0/R_{lc}$	Lengthscale of the bulk $\gamma$ -ray emission, Eq. (2)	$10^{-4}$ – $10^0$	fit
$N_0$	Effective number of particles, Eq. (2)	$10^{27}$ – $10^{34}$	fit
$\eta$	Radius of curvature position-dependence, $r_c(x) = R_{lc} (x/R_{lc})^{\eta}$	0.2–1.0	fixed to 0.5
$b$	Magnetic field position-dependence, $B(x) = B_s (R_*/x)^b$	2–3	fixed to 2.5
$x_{in}/R_{lc}$	Inner gap location	0.2–1.0	fixed to 0.5
$x_{out}/R_{lc}$	Outer gap location	1.0–2.0	fixed to 1.5
$\Gamma_{in}$	Particle Lorentz factor at birth	$10^3$ – $10^4$	fixed to $10^3$
$\alpha_{in}$	Particle pitch angle at birth	$0$ – $\pi/2$	fixed to $\pi/4$

} Proven to be secondary or irrelevant parameters in fitting

- We consider spectra in the 2nd Fermi Pulsar catalog (117 objects)
  - With 5 consecutive data points (81 pulsars)
    - 59 young pulsars (YPs) and 22 MSPs ( $P=1.5 - 22$  ms)
- We apply the model without differentiating between MSPs and YPs, or radio loudness

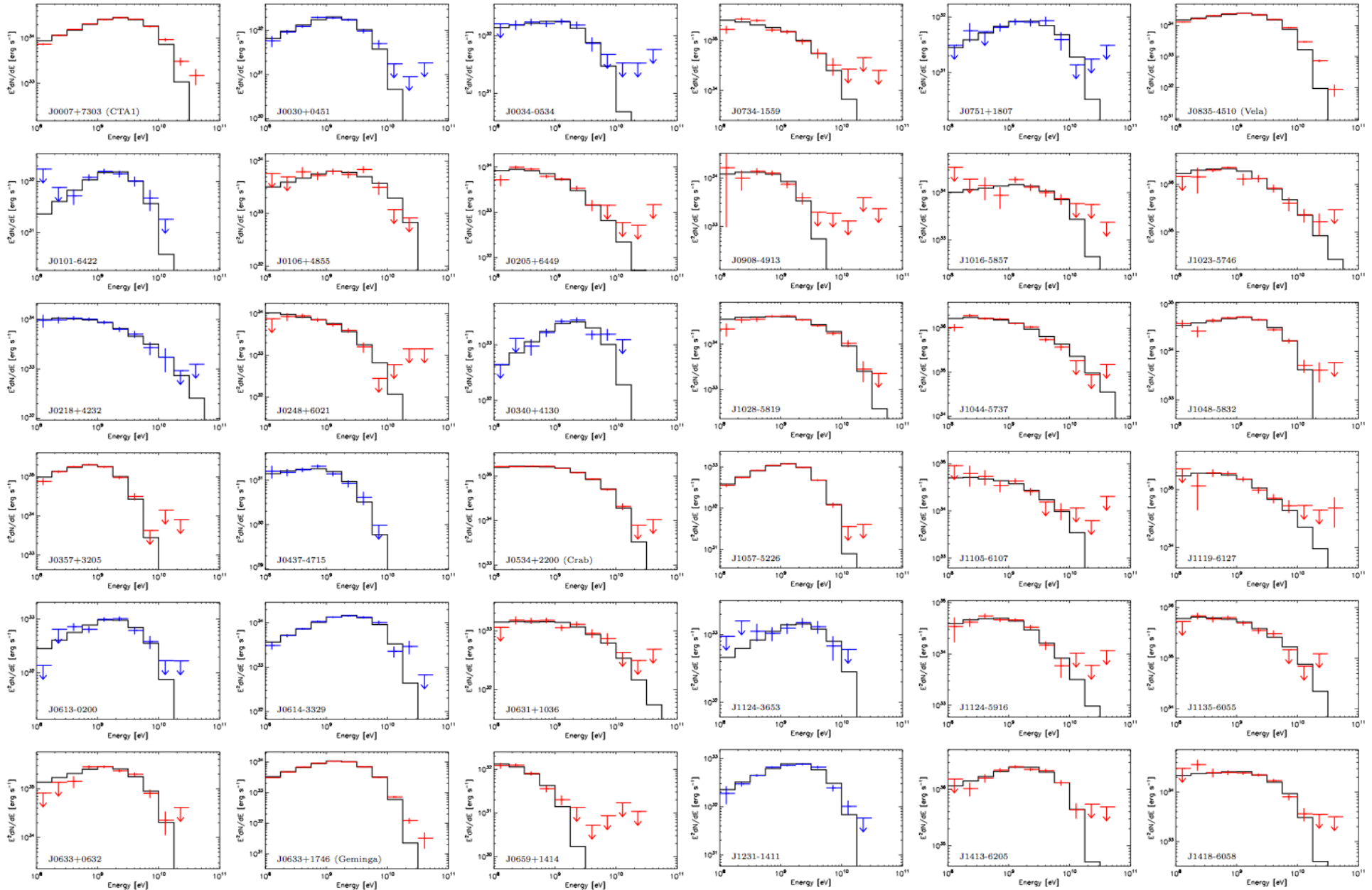


## An iterative procedure: thousands of models per pulsar



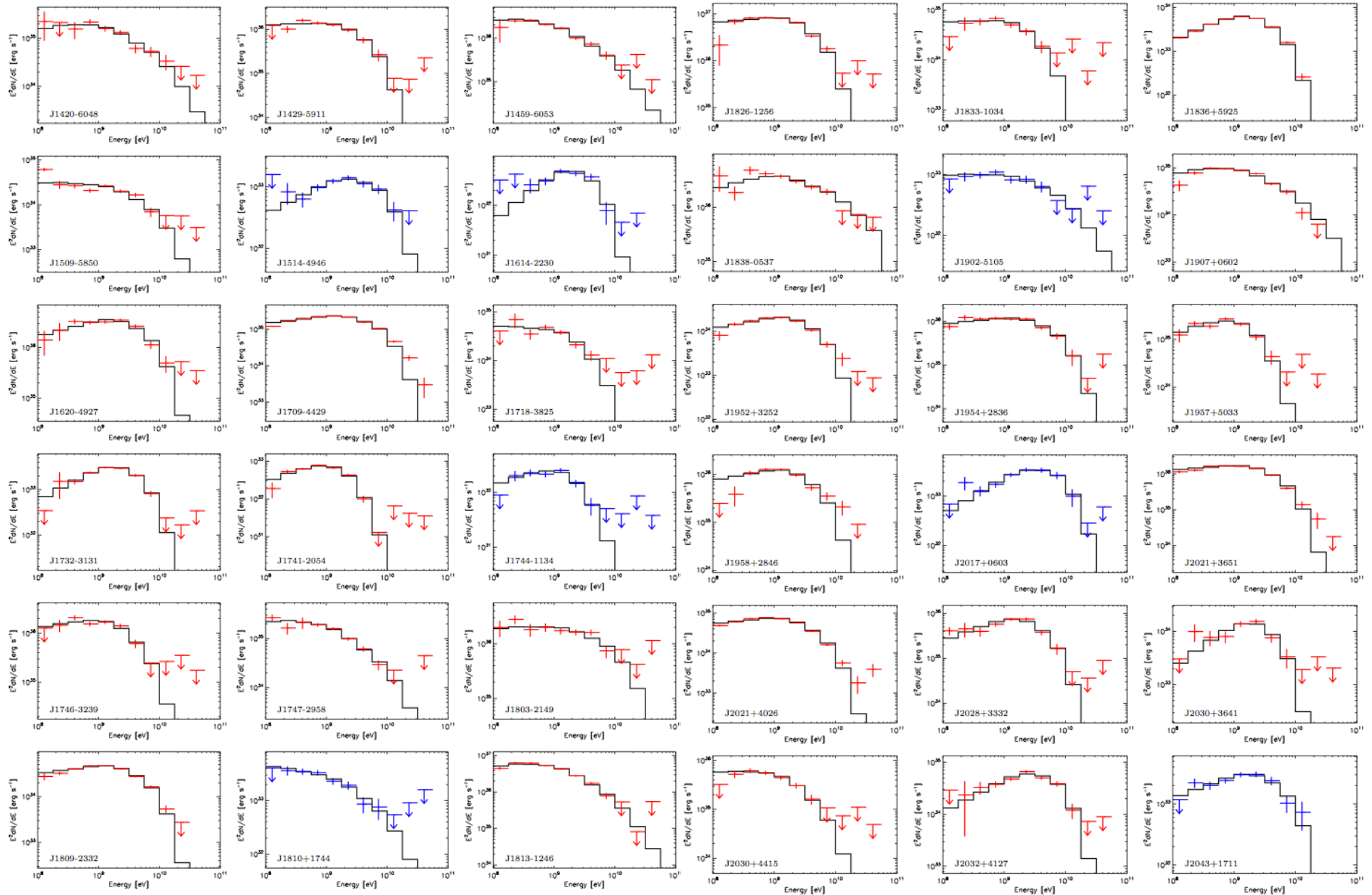


# Spectral fittings of all well-measured Fermi-LAT pulsars in the 2PC



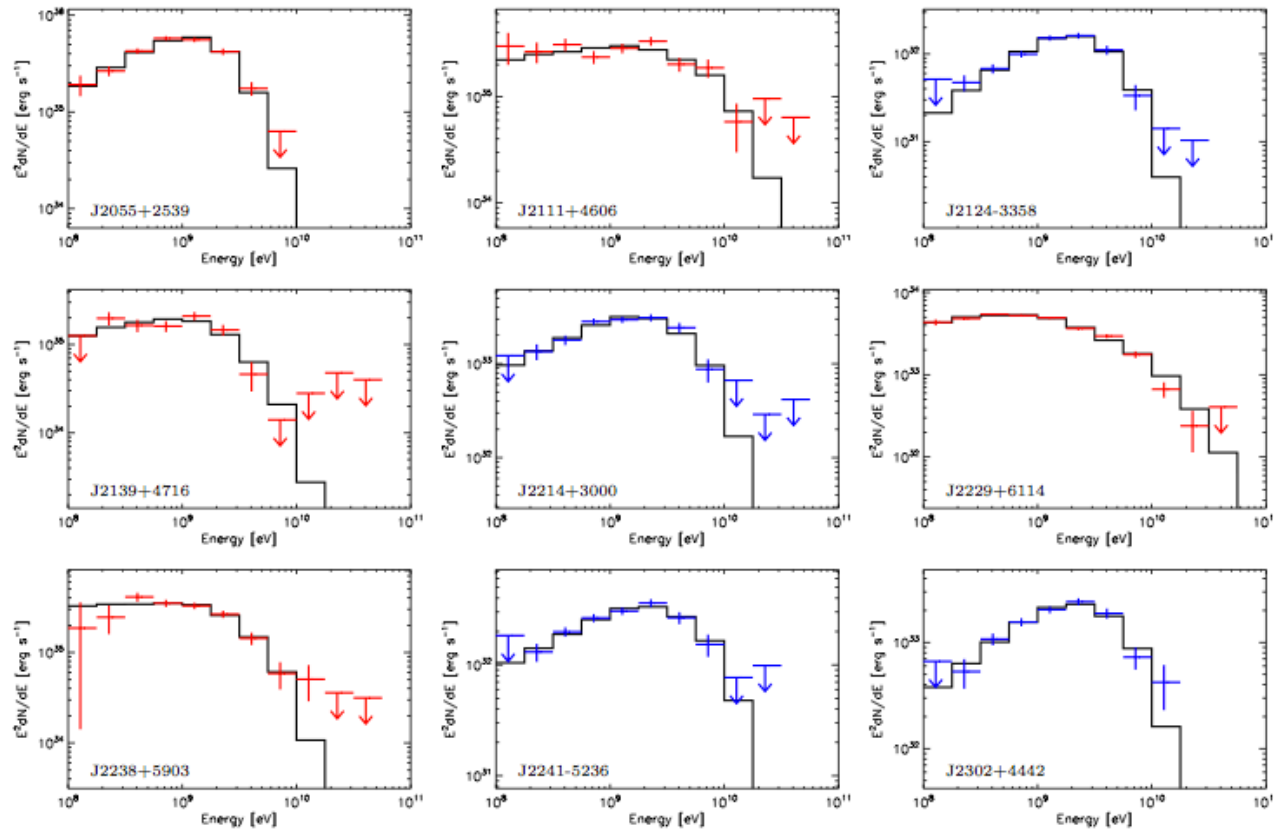


# Spectral fittings of all well-measured Fermi-LAT pulsars in the 2PC





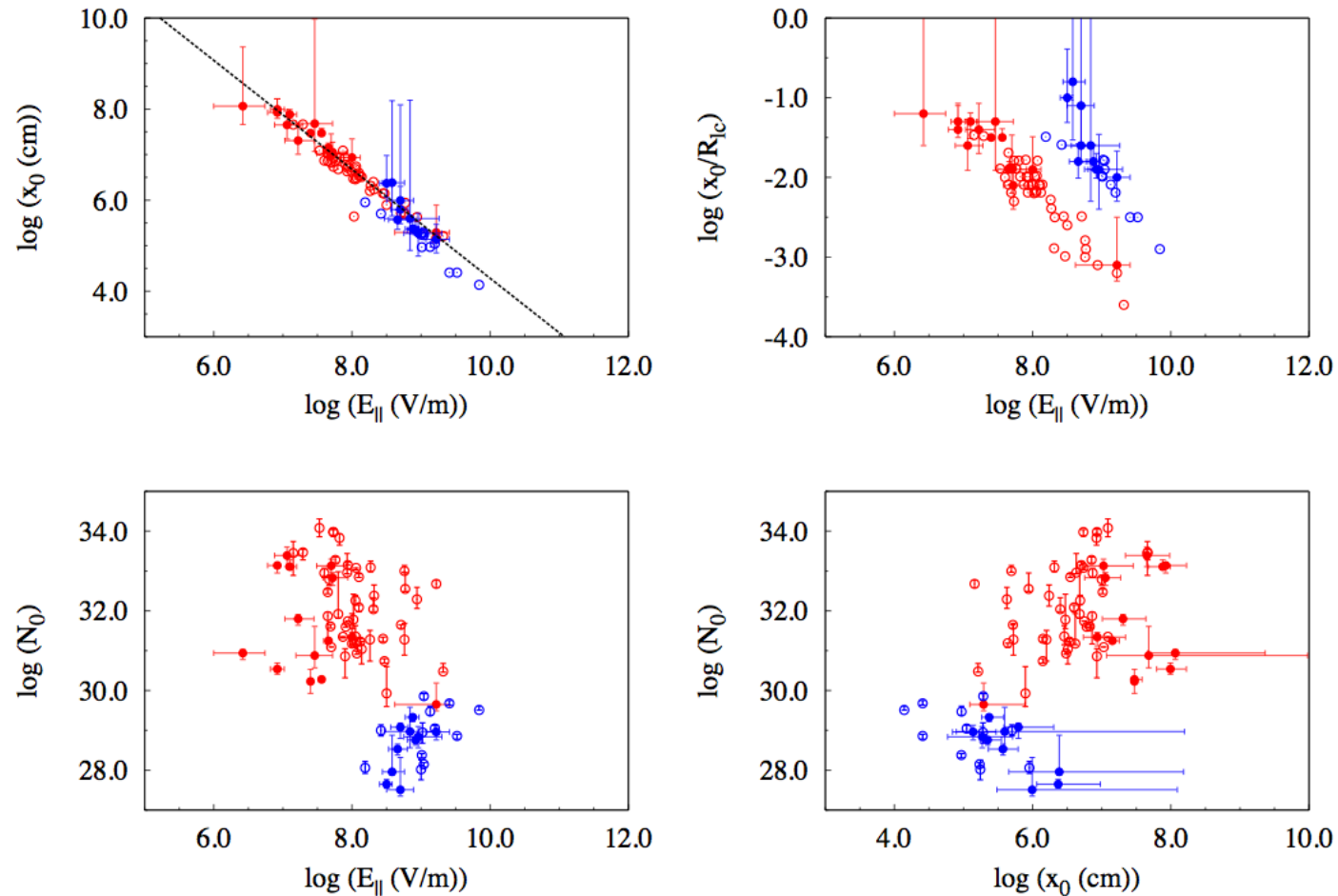
# Spectral fittings of all well-measured Fermi-LAT pulsars in the 2PC



- With 3 parameters, the model copes well with data of dozens of pulsars (YP or MSP)
- The accelerating electric field is of the order of  $10^8$  V/m for YPs, and  $10^9$  V/m for MSPs.
- The value of  $x_0$  range from a few to hundreds of km, which represent a small fraction of the corresponding magnetospheric sizes ( $x_0/R_{lc} \sim 10^{-4} - 10^{-1}$ ).



## Self-correlation of fitting parameters

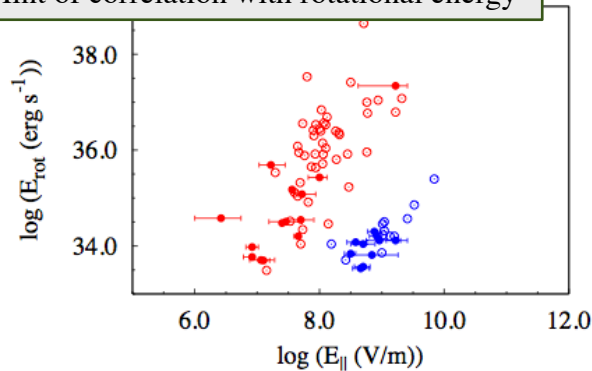


- All three parameters roughly separates between YPs and MSPs
- $E_{||}$  anti-correlates with  $x_0$ 
  - MSPs need larger values of  $E_{||}$  to compensate for a smaller radius of curvature (due to the much closer light cylinder), and make the particles energetic enough ( $\Gamma \sim 10^7$ - $10^8$ ) as to be able to produce  $\sim$  GeV photons
  - Given that their spectra are flat at low Fermi-LAT energies, lower values of  $x_0$  are needed

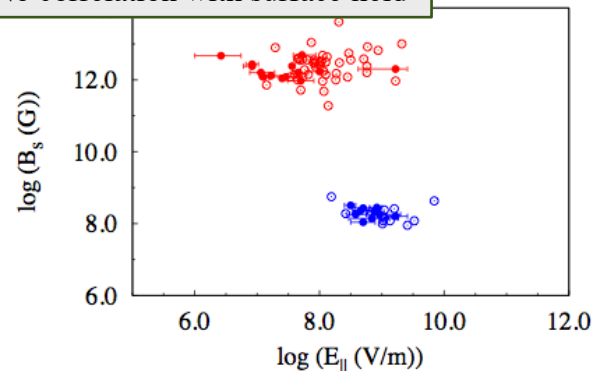


# Correlation with timing parameters: the gaps are far from the NS

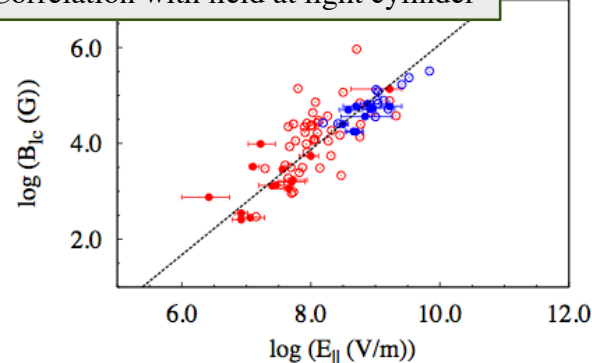
Hint of correlation with rotational energy



No correlation with surface field



Correlation with field at light cylinder



- Hint of a correlation linking  $E_{\parallel}$  with the spin-down power
- No correlation with  $B_s$
- Strong correlation of  $E_{\parallel}$  with the magnetic field at light cylinder,  $B_{lc}$ .
- Such  $E_{\parallel}$ - $B_{lc}$  correlation quantitatively unifies under the same trend the two sub-classes, YPs and MSPs
  - $E_{\parallel}$  is larger in MSPs because their light cylinders are much closer to the surface than they are for YPs
  - If we extrapolate the correlation  $E_{\parallel}(B_{lc})$  to the magnetar regime ( $B_{lc} \sim 10^{-1}-10^2$  G),  $E_{\parallel}$  would be very weak,  $E_{\parallel} < 10^6$  V/m, and unable to provide particles energetic enough as to emit  $\gamma$ -rays.



## Conclusions

- A synchro-curvature model was applied to Fermi-LAT spectral data
  - Model is simple enough as to deal with direct fitting of many sources
  - But recall that it:
    - Contains no geometry (1D)
    - Assumes an *effective* particle distribution fitting their parameters
    - No lightcurve modelling
  - Only 3 fit parameters for all pulsars:  $E_{\parallel}$ ,  $N_0$ , and  $x_0$
- The best-fit models are consistent with significant radiation coming from the initial part of the particle trajectories ( $x_0 \ll R_{lc}$ ), where the perpendicular momentum is not negligible and the losses are dominantly synchrotron-like ( $\xi \gg 1$ ).

Model details in  
Viganò & DFT, 2015 MNRAS (arXiv 1503.04060)











# Parameters (\*)

MODEL PARAMETERS USED TO MODEL THE SED OF PSR J1023+0038 AND XSS J12270-4859.

$\xi$	$k_{ej}$	$\omega_*$	$R_{in}$ (km)	$\bar{B}$ (MG)	$\dot{M}$	$L_{prop}$	$n_e$ ( $10^{18} \text{ cm}^{-3}$ )	$V$ ( $10^{15} \text{ cm}^3$ )	$L_{SSC}/L_{sync}$	$L_{accr}^X$	$\eta_{accr}^X$
PSR J1023+0038											
0.15	0.99	1.50	31.2	2.6	2.7	1.96	54	$6 \times 10^{-4}$	5.0	0.65	0.06
0.15	0.99	1.75	34.6	1.9	1.9	2.23	10	0.01	2.8	0.59	0.08
0.15	0.99	2.00	37.8	1.5	1.4	2.43	5.0	0.04	2.4	0.55	0.11
0.15	0.99	2.25	40.9	1.15	1.1	2.56	2.1	0.19	2.04	0.51	0.14
0.15	0.99	2.50	43.8	0.94	0.8	2.62	1.3	0.50	1.9	0.48	0.17
XSS J12270-4859											
0.15	0.99	2.50	43.8	1.34	2.4	2.62	1.7	0.21	2.2	0.55	0.08

NOTE. — Input parameters are listed in the leftmost three columns. Physical quantities obtained using the analytical relations given in text, are listed in columns 4-8. Parameters estimated from the modelling of the observed SED are given in the five rightmost columns. Luminosities are given in units of  $10^{34} \text{ erg s}^{-1}$ , while the mass in-flow rate is expressed in units of  $10^{-11} M_{\odot} \text{ yr}^{-1}$ .



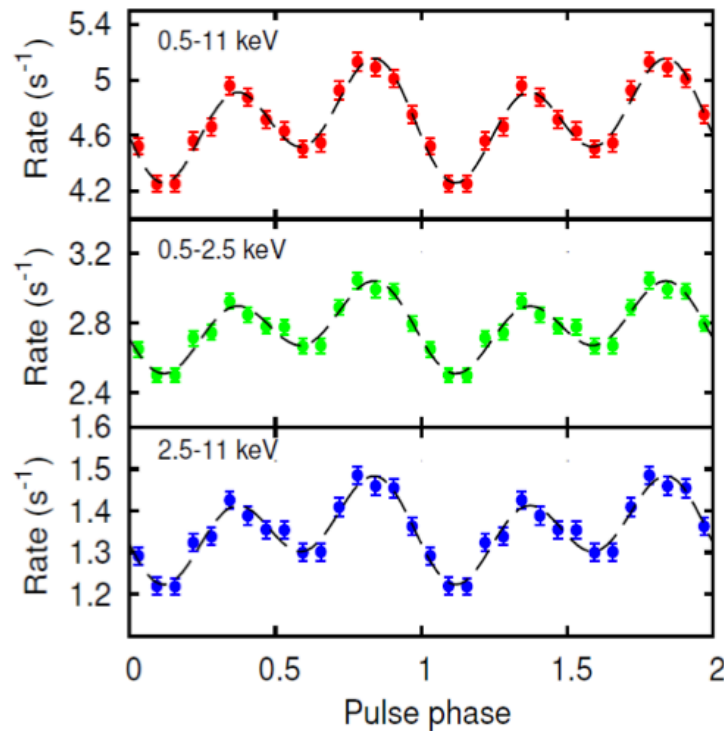
## The sub-luminous disk state showed by the transitional PSRs

- **Presence of an accretion disk:** H $\alpha$  broad, sometimes double peaked emission lines observed in the optical spectrum (Wang et al. 2009; Pallanca et al. 2013; Halpern et al. 2013; De Martino et al. 2014)
- **Average X-ray luminosity  $10^{33}$  to  $10^{34}$  erg s $^{-1}$** , intermediate between the peak of X-ray outbursts ( $10^{36}$  erg s $^{-1}$ ) and the rotation powered emission ( $<10^{32}$  erg s $^{-1}$ );
  - the X-ray emission is variable on timescales of few tens of seconds and has a spectrum described by a power-law with index  $\Gamma \simeq 1.5$  and no cut-off below 100keV (Saitou et al. 2009; De Martino et al. 2010, 2013; Papitto et al. 2013; Linares et al. 2014; Patruno et al. 2014; Tendulkar et al. 2014)
- **0.1-10 GeV luminosity of  $\approx 10^{34}$  erg s $^{-1}$** , 10x brighter with respect to the level observed during the rotation powered state (De Martino et al. 2010; Hill et al. 2011, Papitto, DFT & Li 2014, Stappers et al. 2014; Takata et al. 2014). Transitional pulsars are the only low-mass X-ray binaries from which a gamma-ray emission has been detected so far by Fermi/LAT.
- **a bright, flat-spectrum radio emission indicative of partially absorbed synchrotron emission;** transitional ms pulsars in this state are 1-2 orders of magnitude brighter at radio frequencies with respect to the extrapolation of the radio/X-ray correlation observed from X-ray brighter NS (Deller et al. 2014).
- **Presence of accretion-driven X-ray coherent pulsations** at an rms amplitude btw 5 and 10 per cent, detected from the two sources that were observed at a high-enough temporal resolution, PSR J1023+0038 and XSS J12270-4859 (Archibald et al. 2014, Papitto et al. 2015)

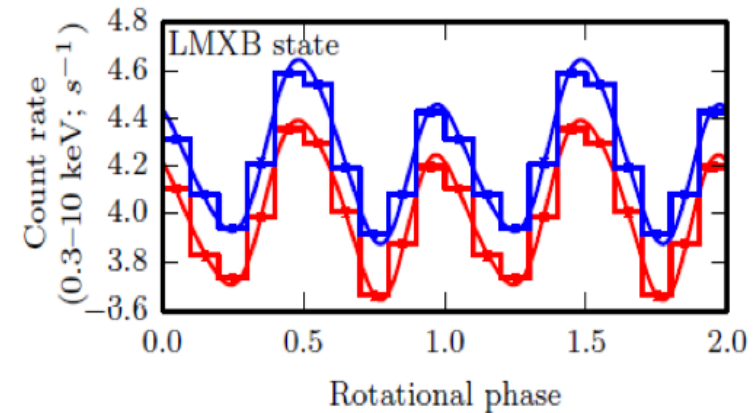


# Detection of X-ray pulsations during sub-luminous state

XSS J12270-4859  
Papitto et al. 2015



PSR B1023+0038  
Archibald et al. 2015



Coherent pulsations with rms amplitude  $\sim 10\%$

Pulsed flux  $\sim 10$  times larger than during radio pulsar state  $\rightarrow$  accretion powered pulsations

X-ray luminosity  $\sim 1000$  times lower than in accreting ms pulsars

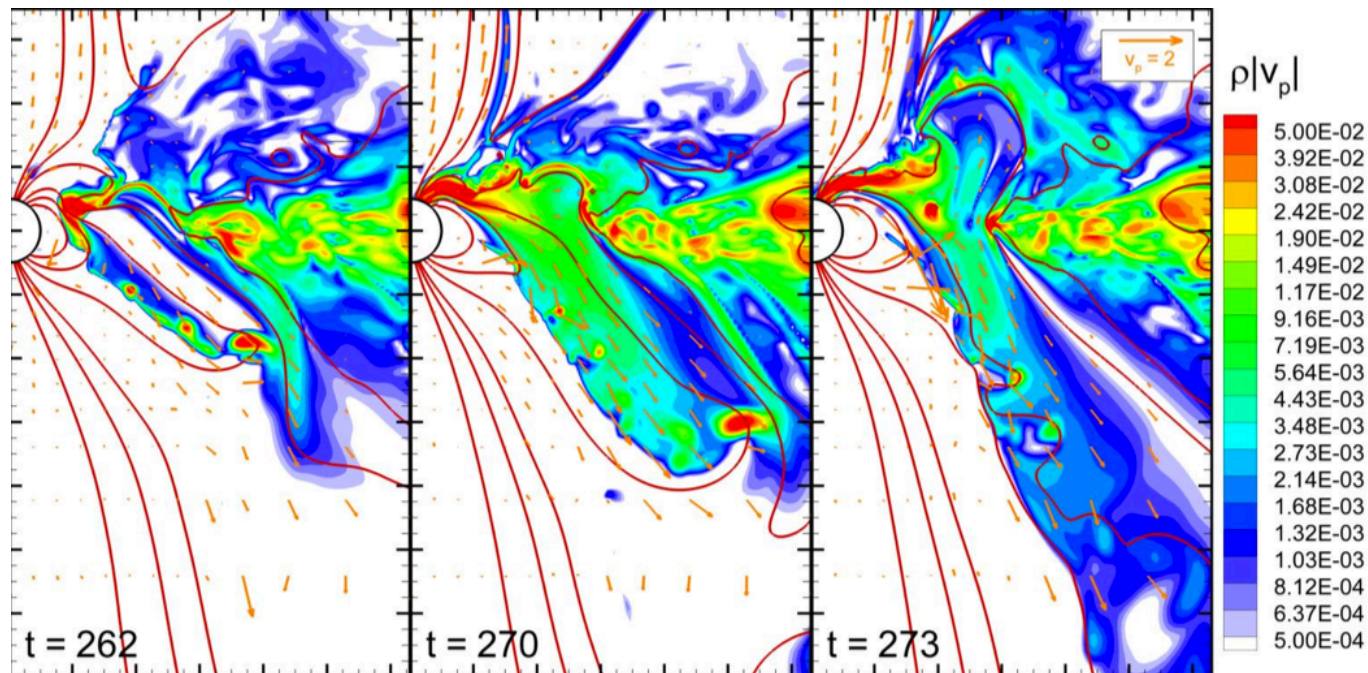


## Propeller outflows can co-exist with partly accreted matter

Lii, Romanova+ 2014 showed in MHD simulations that when the centrifugal barrier is surpassed, matter enters into the magnetosphere. Part is accreted, part is launched in an outflow.

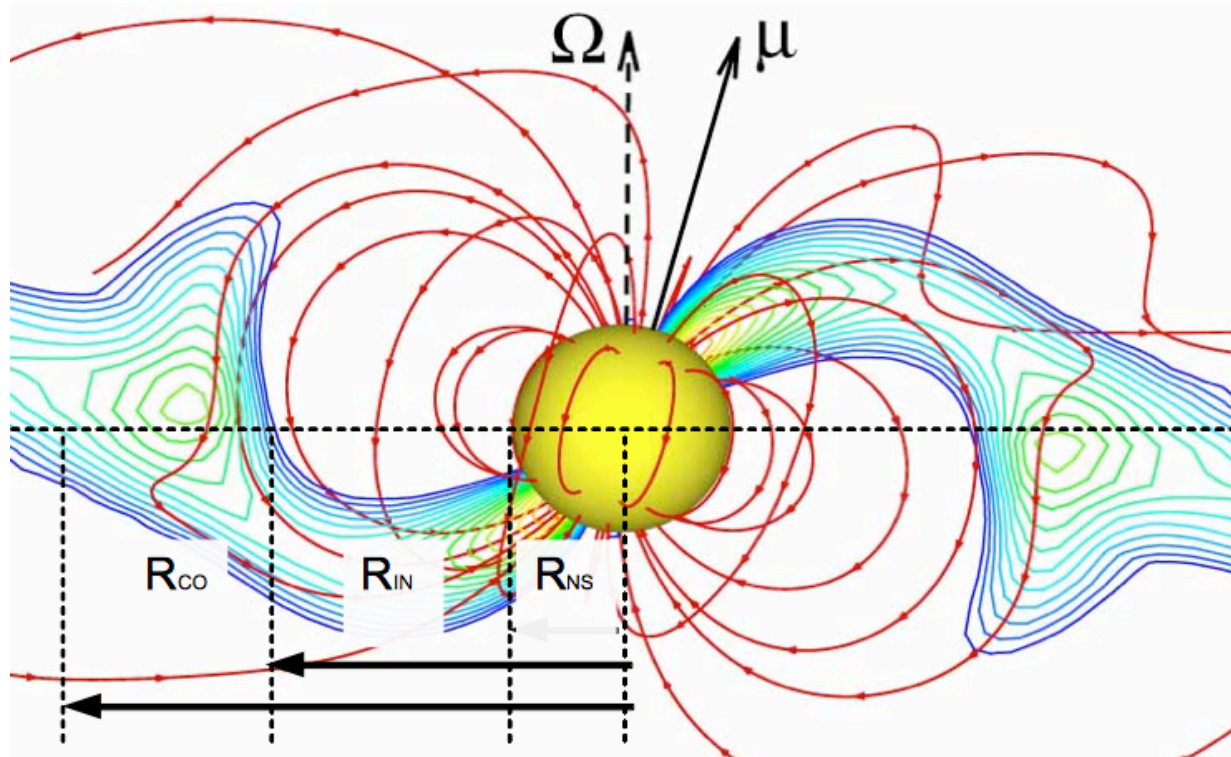
### Accretion and outflows can coexist

The larger the fastness, the larger is the fraction of the mass that is ejected





## Limits to accreted matter flow from the detection of pulses



The mass accretion rate on the NS surface is 100 times smaller than the one required to keep the magnetosphere inside the corotation radius

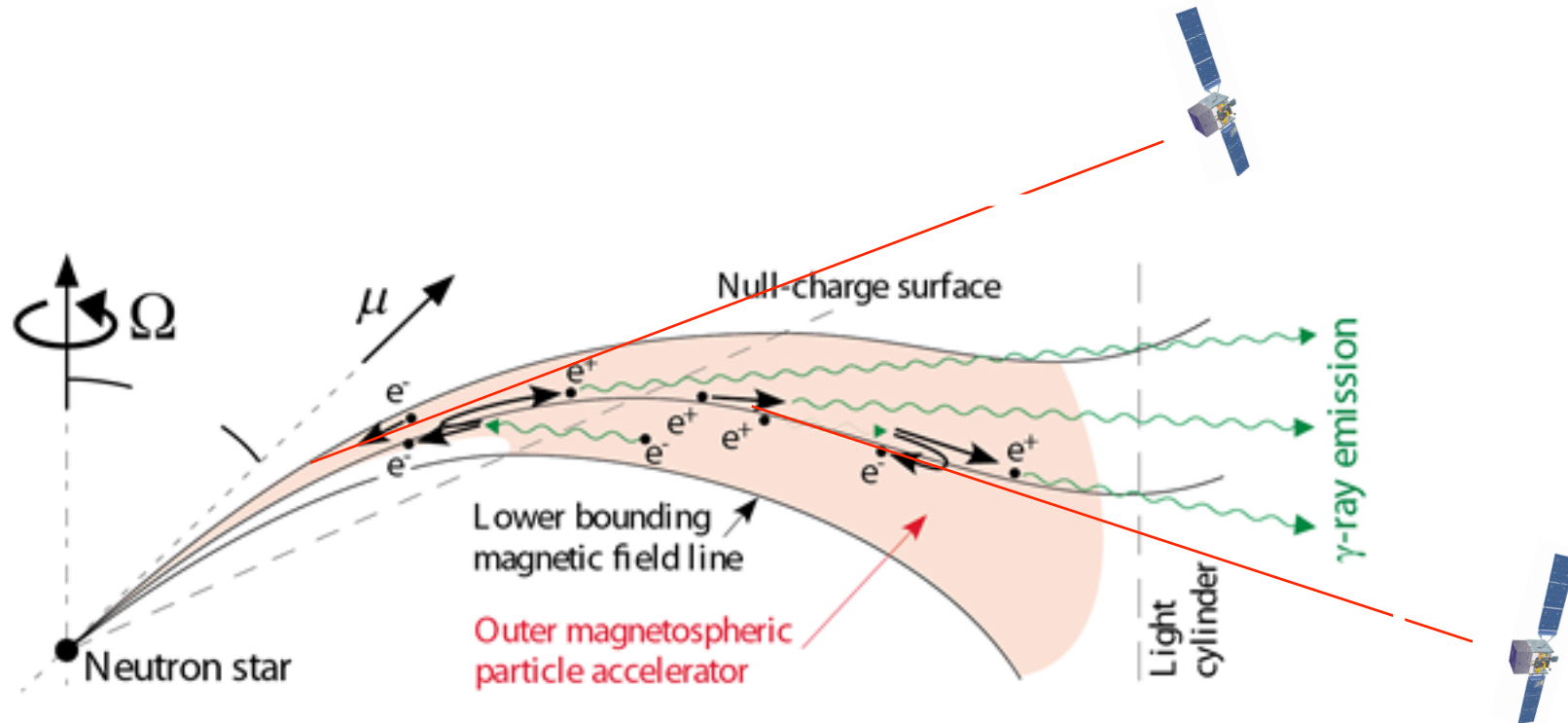
$$(dM/dt)_{NS} \sim 10^{-2} (dM/dt)_{disk}$$





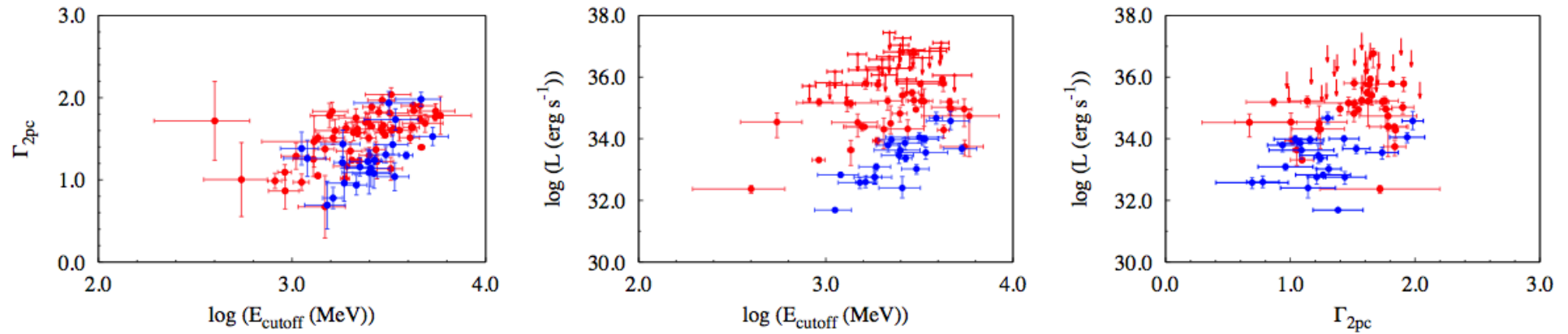


# Geometry and particles moving towards the observer





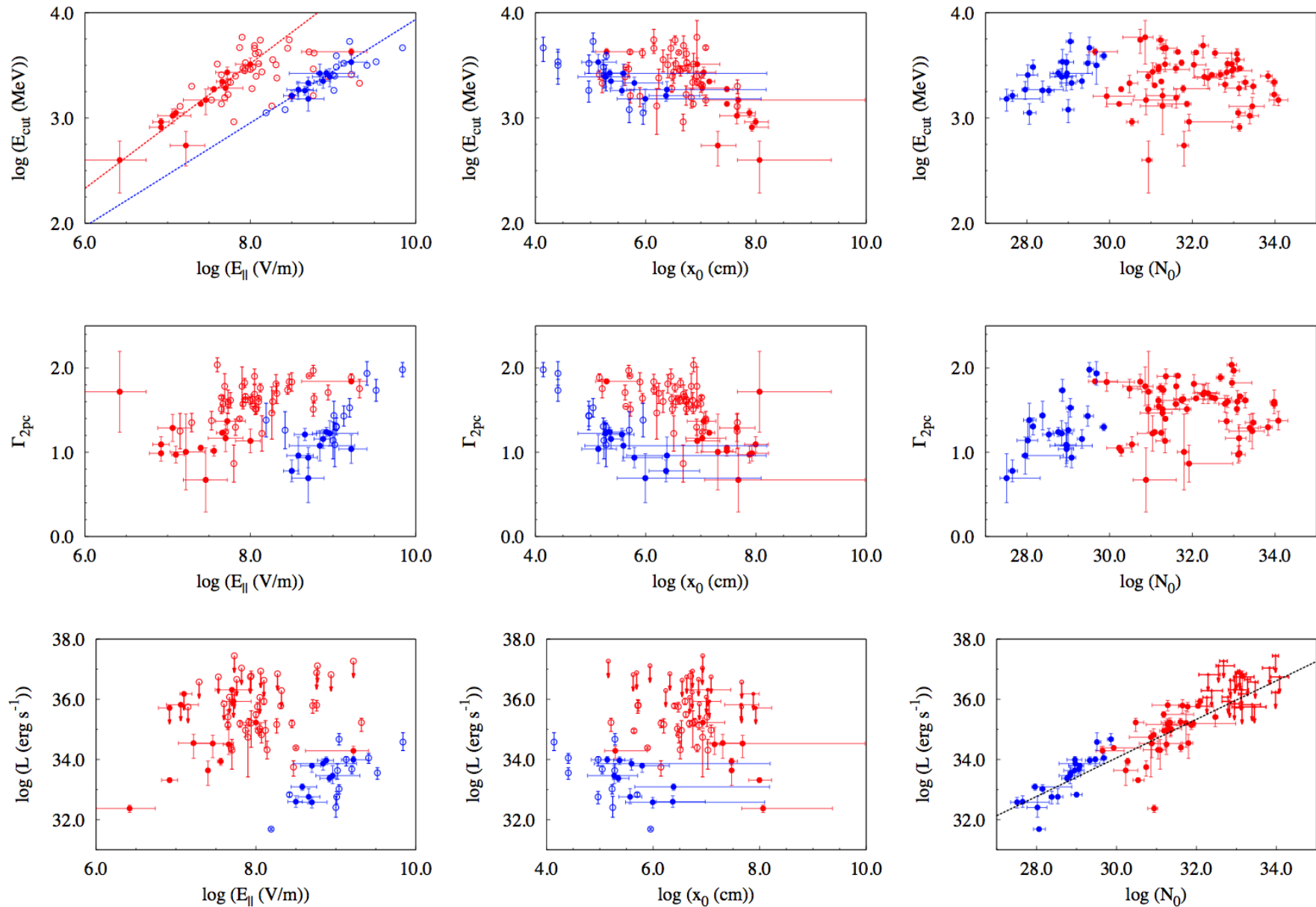
## PLEC parameters do not show any self-correlation



-Nor they separate the sample (except for the luminosity)



# PLEC parameters are not easily associated with SC ones





## Degeneracy in determining best fit models

$$\frac{d(p \sin \alpha)}{dt} = -\frac{P_{sc} \sin \alpha}{v},$$
$$\frac{d(p \cos \alpha)}{dt} = eE_{\parallel} - \frac{P_{sc} \cos \alpha}{v}$$

When the acceleration dominates over the SC power,  $eE_{\parallel} \gg P_{sc} \cos \alpha/v$ , one can simplify the eq. of motion considering also that  $\cos \alpha \rightarrow 1$  very fast, as seen in the numerically computed trajectories.

Then,  $d\Gamma/dt \sim eE_{\parallel}/mv \sim \text{constant}$  in the acc. regime

In other words, the linear rise of the trajectory ( $\Gamma(x)$ ) can be displaced to lower  $x$  by rising the value of  $E_{\parallel}$ .

In many pulsars with relatively flat slopes, this part of the trajectory is dominating the spectrum, and the best-fitting models are endowed with a value of  $x_0$  smaller than the distance at which saturated values of  $\Gamma$  are reached.

Therefore, the best-fitting solutions is degenerate: larger  $E_{\parallel}$  can be compensated by rescaling  $x_0$  with  $1/E_{\parallel}$  in an individual pulsar.

Such argument explains the individual degeneracy appearing in some of the contour plot of  $\chi^2$ , but not the similar global trend found when comparing the best-fitting parameters for all pulsars, i.e., again,  $E_{\parallel} \sim 1/x_0$